

Structure and Depletion at Fluorocarbon and Hydrocarbon/Water Liquid/Liquid Interfaces

Kaoru Kashimoto,^{1,2} Jaesung Yoon,¹ Binyang Hou,¹ Chiu-hao Chen,¹ Binhua Lin,³
Makoto Aratono,² Takanori Takiue,² and Mark L. Schlossman^{1,*}

¹*Department of Physics, University of Illinois at Chicago, Chicago, Illinois 60607, USA*

²*Department of Chemistry and Physics of Condensed Matter, Graduate School of Sciences, Kyushu University, Fukuoka 812-8581, Japan*

³*The Center for Advanced Radiation Sources, University of Chicago, Chicago, Illinois 60637, USA*

(Received 29 April 2008; published 14 August 2008)

The results of x-ray reflectivity studies of two oil/water (liquid/liquid) interfaces are inconsistent with recent predictions of the presence of a vaporlike depletion region at hydrophobic/aqueous interfaces. One of the oils, perfluorohexane, is a fluorocarbon whose superhydrophobic interface with water provides a stringent test for the presence of a depletion layer. The other oil, heptane, is a hydrocarbon and, therefore, is more relevant to the study of biomolecular hydrophobicity. These results are consistent with the subangstrom proximity of water to soft hydrophobic materials.

DOI: [10.1103/PhysRevLett.101.076102](https://doi.org/10.1103/PhysRevLett.101.076102)

PACS numbers: 68.05.-n, 61.05.cm, 82.70.Uv

The formation of a vaporlike depletion layer at the interface between an aqueous solution and a hydrophobic material would have important consequences for many biological, chemical, and environmental processes. Such a layer would limit water molecules, and solutes in the water, from being positioned immediately adjacent to a hydrophobic material. This would affect dynamic processes such as protein folding and self-assembly in which hydrophobic regions are briefly exposed to water, as well as the wetting of aqueous solutions on many environmental and industrially important surfaces.

Early theoretical studies indicated that water maintains a hydrogen bond network surrounding small hydrophobic solutes, though this network would be stretched with increasing solute size [1]. For an infinite radius solute, or equivalently for a planar interface, Stillinger predicted the existence of a depletion layer that is essentially a water-vapor interface that forms near the hydrophobic plane [1]. Recent theory and computer simulations suggest the presence of a depletion layer whose thickness is on the order of a few angstroms for solutes of several nanometers or larger radius [2–6]. Attractive interactions between the hydrophobic material and water are expected to thin the depletion layer [3,7]. Recent simulations of planar interfaces that include attractive interactions have suggested that a master curve describes the variation of the depletion layer thickness with surface hydrophobicity [6].

Numerous experimental studies have provided conflicting evidence for and against the presence of a depletion layer [8–19], though recent x-ray and neutron scattering studies from the interface between water and a hydrophobic coating on a solid provide evidence for a depletion layer with thickness of a few angstroms [13–15,17]. Since biological hydrophobic/aqueous interfaces are often soft, there is a need for studies of soft and well-defined hydrophobic/aqueous interfaces. Recent optical ellipsometry

studies of liquid/liquid interfaces were analyzed by one of two models that yielded a range of depletion layer thickness values that varied from 0.3 to 3 Å for the same sets of data [12]. Also of interest are vibrational sum frequency spectroscopy studies that demonstrate much weaker hydrogen bonding in the region of the water/hydrophobic liquid interface than at the water/vapor interface [20]. These data suggest that a bulklike water/vapor interface does not form near a water/hydrophobic liquid interface. However, the lack of depth sensitivity in the spectroscopy measurements preclude them from providing a decisive argument for or against the existence of depletion layers. Here, we present x-ray reflectivity studies of two oil/water (liquid/liquid) interfaces. One of these interfaces, the perfluorohexane/water interface, is superhydrophobic and, therefore, provides a stringent test of the depletion layer prediction. The other is a hydrocarbon (heptane)/water interface that is more relevant to the study of biomolecular hydrophobicity. The materials used for these studies were extensively purified and their purity was tested with tensiometry and gas-liquid chromatography (see supplementary information [21] for a detailed description).

Teflon and other fluorocarbon materials are strongly hydrophobic. The superhydrophobicity of the interface between liquid perfluoro-*n*-hexane [CF₃(CF₂)₄CF₃] and water at 23.5 °C is evident in Fig. 1 which shows a spherical drop of water in equilibrium at the perfluorohexane/air interface. The dihedral angle is 180° to within our measurement accuracy ($\pm 1^\circ$). This is consistent with the large, negative spreading coefficient of -110.7 mN m^{-1} determined by our measurements of interfacial tension, which indicates that water does not wet perfluorohexane (see supplementary information [21]).

X-ray reflectivity probes the electron density variation with interfacial depth. Figure 2 illustrates reflectivity data

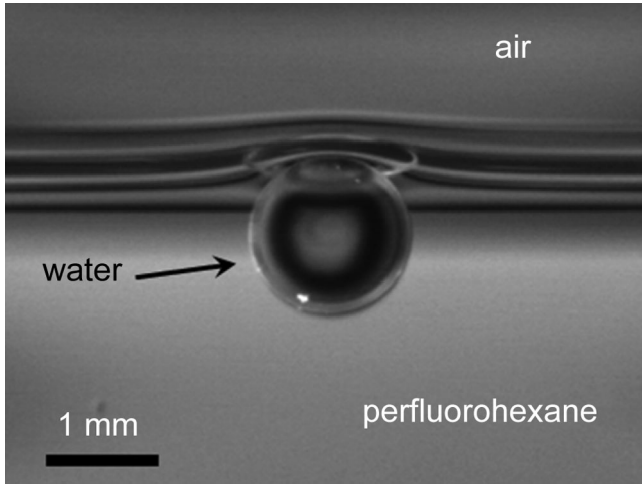


FIG. 1. Water drop placed at the perfluorohexane/air interface.

$R(Q_z)$ as a function of the wave vector transfer Q_z (normal to the interface) from a flat, circular perfluorohexane/water interface of 70 mm diameter [21]. The reflectivity was determined by measurements of the reflected x-ray intensity normalized by the incident intensity, after subtraction of background scattering [21–23]. The reduction of the measured reflectivity below the calculated Fresnel reflectivity

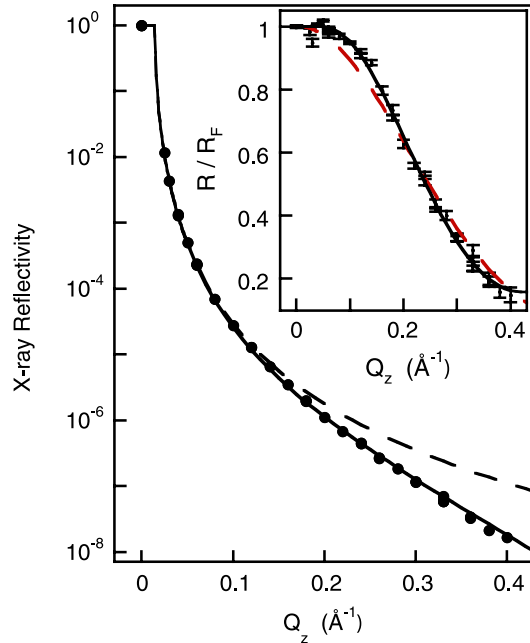


FIG. 2 (color online). X-ray reflectivity from the perfluorohexane/water interface at 23.5 °C as a function of wave vector transfer normal to the interface. Solid line: fit to capillary wave theory. Dashed line: Fresnel reflectivity R_F . Error bars are smaller than the symbols. The point at $Q_z = 0$ is the direct (not reflected) beam that is used to normalize the reflectivity. Inset: X-ray reflectivity normalized to R_F . Dashed (red) line: Fit to capillary wave theory. Solid line: Fit to perfluorohexane multilayering.

tivity $R_F(Q_z)$ expected from an ideal, smooth interface (see Fig. 2) can be described by [24]

$$R(Q_z) \approx R_F(Q_z) \exp(-Q_z Q_z^T \sigma^2), \quad (1)$$

where $Q_z^T \approx \sqrt{Q_z^2 - Q_c^2}$ is the wave vector transfer in the lower (e.g., perfluorohexane) phase and the critical wave vector transfer for total x-ray reflection is calculated to be $Q_c = 0.01458 \text{ \AA}^{-1}$ for perfluorohexane/water and $Q_c = 0.01169 \text{ \AA}^{-1}$ for heptane/water interfaces [21]. The interfacial width σ describes the crossover from one bulk phase to the other via an error function, $\text{erf}(z/\sqrt{2}\sigma)$ (see supplementary information [21]). A two parameter fit of the reflectivity data yields $\sigma = 3.4 \pm 0.2 \text{ \AA}$ and $Q_{\text{offset}} = 0.0004 \text{ \AA}^{-1}$, where the latter is an additive offset in Q that represents a typical misalignment of the x-ray instrument. This fit produces the solid line that is in good agreement with the data in Fig. 2. Although Eq. (1) does not include the resolution dependent contribution from capillary waves, this is a small effect for these experiments (because $\eta \leq 0.2$, see [25,26]).

Capillary waves at the interface, driven by thermal energy, will scatter x rays out of the specularly reflected beam and reduce the measured reflectivity below the Fresnel reflectivity [27]. Hybrid capillary wave theory describes the total interfacial width as $\sigma^2 = \sigma_{\text{cap}}^2 + \sigma_{\text{int}}^2$ [28]. The intrinsic width σ_{int} represents the effect of interfacial molecular ordering and σ is a result of the intrinsic profile fluctuating according to the capillary wave spectrum. Capillary wave theory predicts $\sigma_{\text{cap}} = 3.37 \text{ \AA}$ (see supplementary information [21]), in agreement with our measurement of σ . Therefore, σ_{int} is small, suggesting that the intrinsic molecular ordering at the interface is weak.

The high accuracy of the data in Fig. 2 allows us to present them in the inset to Fig. 2 as reflectivity normalized to the Fresnel reflectivity $R(Q_z)/R_F(Q_z)$. This reveals small but significant deviations of the data from the fit to Eq. (1). As described shortly, these deviations cannot be explained by a depletion layer (or by any single layer, see supplementary information [21]). Although these data cannot uniquely specify the molecular origin of this effect, they can be modeled by multiple layering of perfluorohexane molecules at the interface. The fitting shown in the Fig. 2 inset used an intrinsic profile $\langle \rho(z) \rangle_{\text{int}} = \rho_f + A[C - \cos(2\pi z/l_{\text{osc}} + \phi)] \exp(-z/l_{\text{dec}})$, where one period of the cosine represents a layer of perfluorohexane molecules. The fraction of perfluorohexane molecules that form a layer decreases with increasing distance from the interface according to the exponential decay length l_{dec} (supplementary information [21]). This modeling suggests that two to three layers of perfluorohexane exist at the interface, though the maximum density of these layers is only 3% above the bulk liquid perfluorohexane density. Given the rigid, nearly cylindrical shape of perfluorohexane molecules, this layering is reminiscent of

smectic multilayering that occurs at the surface of liquid crystals [29].

Figure 3 demonstrates that the reflectivity data from the perfluorohexane/water interface is inconsistent with the presence of a depletion layer. The interface is modeled by back-to-back water/vapor and vapor/oil interfaces that are separated by a distance D_{dep} (Fig. 3, inset). The electron density profile of this interface is given by

$$\langle \rho(z) \rangle_{xy} = \frac{1}{2} \rho_{\text{water}} \left[1 - \operatorname{erf} \left(\frac{z}{\sqrt{2}\sigma} \right) \right] + \frac{1}{2} \rho_{\text{oil}} \left[1 + \operatorname{erf} \left(\frac{z - D_{\text{dep}}}{\sqrt{2}\sigma} \right) \right]. \quad (2)$$

This model represents a depletion layer of vaporlike density and thickness D_{dep} sandwiched between bulk water and oil. The water/vapor and vapor/oil interfaces fluctuate with capillary waves, as represented by the error function in Eq. (2). We let $\sigma = 3.4 \text{ \AA}$, as determined by the x-ray measurements. It could be argued that a vaporlike depletion layer will have interfacial widths characteristic of the bulk water/vapor and vapor/oil interfaces, but the data cannot be fit with such values for the widths [21]. The data in Fig. 3 are sensitive to the presence of depletion layers of 0.2 \AA thickness and exclude any such layer of this thickness or greater. This is generally much thinner than depletion layers previously reported.

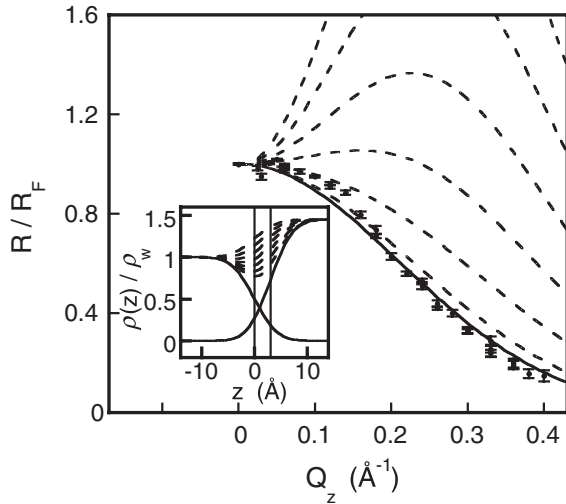


FIG. 3. Depletion layer analysis for the perfluorohexane/water interface. Data from Fig. 2. Solid line: Fit to Eq. (1). Dashed lines: Calculated from Eq. (2) with $D_{\text{dep}} = 0.5$ to 3 \AA in steps of 0.5 \AA (bottom to top) with $\sigma = 3.4 \text{ \AA}$. Inset: Electron density profile normalized to bulk water, $\rho(z)/\rho_w$, that is used to calculate the corresponding x-ray reflectivity. Solid lines: Water and perfluorohexane densities for $D_{\text{dep}} = 3 \text{ \AA}$. The 3 \AA separation between the midpoints of the profiles is shown by vertical lines. Dashed lines: Total profiles for $D_{\text{dep}} = 0$ to 3 \AA in steps of 0.5 \AA (top to bottom), where $D_{\text{dep}} = 0 \text{ \AA}$ corresponds to the solid line in the main figure.

A similar reflectivity measurement and analysis has been carried out for the interface between water and a hydrocarbon, hydrophobic liquid—*n*-heptane [$\text{CH}_3(\text{CH}_2)_5\text{CH}_3$]. The normalized reflectivity $R(Q_z)/R_F(Q_z)$ measured from this interface is shown in Fig. 4. A one parameter fit to Eq. (1) is excellent, with a value of the interfacial width $\sigma = 4.2 \pm 0.2 \text{ \AA}$. The small deviations observed in the fit to Eq. (1) for the perfluorohexane/water interface (Fig. 2, inset, dashed red line) are absent. The heptane molecules are flexible and it is unlikely that they would form smectic layers as our data suggest for the rodlike perfluorohexane molecules. This is supported by our interfacial tension measurements as a function of temperature of a similar system, the hexane/water interface, that indicate that it is slightly more disordered than the perfluorohexane/water interface (the excess interfacial entropy, $\Delta s_{\text{perfluorohexane/water}} = 0.070 \text{ mJ K}^{-1} \text{ m}^{-2}$ and $\Delta s_{\text{hexane/water}} = 0.083 \text{ mJ K}^{-1} \text{ m}^{-2}$ at $25 \text{ }^\circ\text{C}$, see supplementary information [21]).

The interfacial width predicted from capillary wave theory for the heptane/water interface is 3.44 \AA , which is different from the measured value of $4.2 \pm 0.2 \text{ \AA}$. Figure 4 demonstrates that this difference is not due to a depletion layer because the presence of a depletion layer would increase the reflectivity above the measured values, as well as above the values predicted by capillary wave theory. Equation (1) indicates that the larger value of the measured width has the opposite effect. It acts to decrease

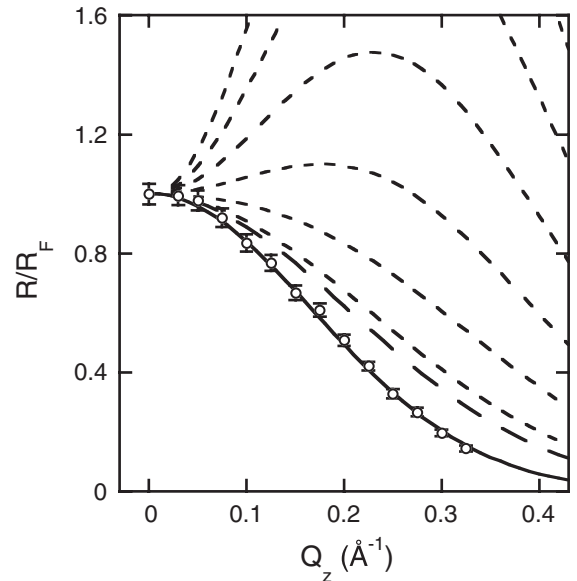


FIG. 4. Depletion layer analysis for the heptane/water interface. Symbols: X-ray reflectivity data at $25 \text{ }^\circ\text{C}$. Solid line: Fit to Eq. (1). Long dashed line: Capillary wave fit with $\sigma_{\text{cap}} = 3.44 \text{ \AA}$. Short dashed lines: Calculated from Eq. (2) with $D_{\text{dep}} = 0.5$ to 3 \AA in steps of 0.5 \AA (bottom to top) with $\sigma_{\text{cap}} = 3.44 \text{ \AA}$. Data point at $Q_z = 0$ is the direct (not reflected) beam.

the reflectivity below the values predicted by capillary wave theory.

Measured values of interfacial width larger than those of the capillary wave prediction have been reported for the liquid alkane/water interface for a range of alkane chain lengths from 6 to 22 carbons [30]. For the reasons just described, the presence of a depletion layer [as in Eq. (2)] cannot explain these variations. A larger interfacial width could be due to the presence of molecular ordering at the interface that leads to an intrinsic width σ_{int} such that the total width $\sigma^2 = \sigma_{\text{cap}}^2 + \sigma_{\text{int}}^2$ is increased. A phenomenological explanation suggested that the intrinsic width was given by the shorter of two relevant length scales that describe alkane ordering: the radius of gyration of the alkane and the bulk correlation length in the alkane liquid [30]. Although this explanation described quantitatively the linear increase in σ with chain length for alkanes of length 6 to 16 carbons, and the constant value for longer alkanes, it did not fully justify that these length scales should characterize the increase in interfacial electron density required to explain the data.

Recent simulations of the hydrophobic/water interface utilized a planar solid surface with a variable hydrophobicity to predict values of the depletion layer thickness to be a few angstroms [6]. Extrapolation of the master curve that resulted from these simulations to a superhydrophobic interface, such as our perfluorohexane/water interface, would predict a depletion layer thickness of ~ 3 Å, in contrast to the upper bound of 0.2 Å determined by our data. With regard to our results on the heptane/water interface, calculations have suggested that attractive van der Waals interactions between a hydrocarbon oil and water will thin the depletion layer to nearly zero thickness [3,7]. Chandler has suggested that the weakness of the attractive van der Waals forces, on the order of $k_B T$, will result in enhanced interfacial fluctuations in the thickness of the depletion layer [31]. Such fluctuations are not included in the capillary wave theory. If present, we anticipate that the interfacial width measured by x-ray reflectivity would increase because x rays would be scattered by the fluctuations. Development of a theory of depletion layer fluctuations, that describes the height-height correlation function of the interface, may help resolve the issue of enhanced interfacial width at the alkane/water interface.

K. K. acknowledges financial support from the Japan Society for the Promotion of Science. M. L. S. acknowledges support from NSF-CHE. ChemMatCARS is supported by NSF-CHE, NSF-DMR, and the U.S. Department of Energy (DOE-BES). The Advanced Photon Source at Argonne National Laboratory and the

National Synchrotron Light Source at Brookhaven National Laboratory are supported by the U.S. DOE-BES.

*schloss@uic.edu

- [1] F. H. Stillinger, *J. Solution Chem.* **2**, 141 (1973).
- [2] L. R. Pratt and A. Pohorille, *Chem. Rev.* **102**, 2671 (2002).
- [3] G. Hummer and S. Garde, *Phys. Rev. Lett.* **80**, 4193 (1998).
- [4] K. Lum, D. Chandler, and J. D. Weeks, *J. Phys. Chem.* **103**, 4570 (1999).
- [5] G. Hummer *et al.*, *Chem. Phys.* **258**, 349 (2000).
- [6] J. Janecek and R. R. Netz, *Langmuir* **23**, 8417 (2007).
- [7] D. M. Huang and D. Chandler, *J. Phys. Chem. B* **106**, 2047 (2002).
- [8] J. W. G. Tyrell and P. Attard, *Phys. Rev. Lett.* **87**, 176104 (2001).
- [9] M. Mao *et al.*, *Langmuir* **20**, 1843 (2004).
- [10] D. A. Doshi *et al.*, *Proc. Natl. Acad. Sci. U.S.A.* **102**, 9458 (2005).
- [11] Y. Takata *et al.*, *Langmuir* **22**, 1715 (2006).
- [12] J. P. R. Day and C. D. Bain, *Phys. Rev. E* **76**, 041601 (2007).
- [13] D. Schwendel *et al.*, *Langmuir* **19**, 2284 (2003).
- [14] A. Poynor *et al.*, *Phys. Rev. Lett.* **97**, 266101 (2006).
- [15] M. Maccarini *et al.*, *Langmuir* **23**, 598 (2007).
- [16] T. R. Jensen *et al.*, *Phys. Rev. Lett.* **90**, 086101 (2003).
- [17] M. Mezger *et al.*, *Proc. Natl. Acad. Sci. U.S.A.* **103**, 18401 (2006).
- [18] S. Subramanian and S. Sampath, *J. Colloid Interface Sci.* **313**, 64 (2007).
- [19] Y.-S. Seo and S. Satija, *Langmuir* **22**, 7113 (2006).
- [20] L. F. Scatena, M. G. Brown, and G. L. Richmond, *Science* **292**, 908 (2001).
- [21] See EPAPS Document No. E-PRLTAO-101-055834 for materials purification, experimental methods, tension and entropy measurements, sample cell design, capillary wave theory calculation, and additional analyses of the x-ray data. For more information on EPAPS, see <http://www.aip.org/pubservs/epaps.html>.
- [22] D. M. Mitrinovic, S. M. Williams, and M. L. Schlossman, *Phys. Rev. E* **63**, 021601 (2001).
- [23] Z. Zhang *et al.*, *J. Chem. Phys.* **110**, 7421 (1999).
- [24] L. Nevot and P. Croce, *Rev. Phys. Appl.* **15**, 761 (1980).
- [25] M. K. Sanyal *et al.*, *Phys. Rev. Lett.* **66**, 628 (1991).
- [26] D. K. Schwartz *et al.*, *Phys. Rev. A* **41**, 5687 (1990).
- [27] A. Braslau, *Phys. Rev. A* **38**, 2457 (1988).
- [28] J. D. Weeks, *J. Chem. Phys.* **67**, 3106 (1977).
- [29] P. S. Pershan, *Faraday Discuss. Chem. Soc.* **89**, 231 (1990).
- [30] D. M. Mitrinovic *et al.*, *Phys. Rev. Lett.* **85**, 582 (2000).
- [31] D. Chandler, *Nature (London)* **445**, 831 (2007).